

# Assessing Crop Water Demand of Wheat Crop in a Canal Command using SEBAL Model

Mamta Rana , D.S. Bundela and R.S. Hooda,

**Abstract:** Crop Actual Evapotranspiration (ET<sub>a</sub>) represents crop water demand and one of the most useful indicators of the amount of water required at different growth periods for its satisfactory growth and optimum production. The overarching goal of this paper was the spatial estimate of water demand of wheat crop in the Hansi Branch Canal Command using high spatial resolution Remote Sensing data. The study used Surface Energy Balance Algorithm for Land (SEBAL) Model to estimate ET spatially from a LANDSAT 7ETM+ image of March 2002. The SEBAL estimated daily ET<sub>a</sub> varies from 0.05 to 3.48 mm/day over the study area. The obtained results for ET<sub>a</sub> were comparable with Pan Evaporation and Penman-Monteith Method estimated ET value. On comparison it is found that the model predicted ET<sub>a</sub> is 15.1% and 50.2% less than ET<sub>c</sub> from the Pan Evaporation Method and Penman-Monteith, respectively.

**Keywords:** Evapotranspiration, Spatial Estimation, SEBAL Model, Remote Sensing, Hansi Branch Canal Command

## 1. INTRODUCTION

India is projected to have a population increase which is highest in the world by 2050, only 40 years from now. Currently, India's population is 12.1 billion and it is likely to grow around 1.36 billion by 2025 and demands 23% increase in agricultural production. This is projected to have a huge impact on its food security. Food security of a country depends on the agricultural production per unit area in cultivable land. Developed countries generally increase agricultural production through better crop varieties and management practices. India made good inroads in the 1960 through the 'green revolution'. However, even though growth of up to 10% is occurring in Information Technology, Manufacturing etc. The agricultural growth is way behind being only 2%. The annual fluctuations in agricultural and food grains production are also very wide. Hence, what are needed are realistic and pragmatic policies which can promote and ensure food security and self-sufficiency in food grains. This underlies the importance of the development of water resources for irrigation in India.

- Mamta Rana is a Senior Research Fellow in the Department of Agromet Services, India Meteorological Department, Lodi Road, New Delhi and pursuing PhD from Centre of Excellence for Energy and Environmental Studies (CEES), Deenbandhu Chhotu Ram University of Science & Technology, Murthal, (Sonapat), Haryana, India. E-mail: [mrana.geo@gmail.com](mailto:mrana.geo@gmail.com).
- D.S. Bundela is a Principal Scientist in the Division of Irrigation & Drainage Engineering, CSSRI, Karnal, Haryana, India.
- R.S. Hooda is Chief Scientist in Haryana Space Application Centre (HARSAC), Deptt. of Science & Technology, Govt. of Haryana, CCS HAU Campus, Hisar, Haryana, India.

Evapo-transpiration (ET) is a key factor for determining crop water demand, for proper irrigation scheduling and for improving water use efficiency in irrigated agriculture. Accurate estimation of evapo-transpiration constitutes an important part of irrigation system planning and designing, and accurate spatial determination is crucial to achieve sustainable agriculture management.

In recent years, several remote sensing methods have been developed (SEBAL, METRIC), which contributed valuable data for irrigation management. Time-Series Remote Sensing data in thermal bands provides an excellent opportunity to estimate surface fluxes on clear-sky conditions for mapping daily evapo-transpiration (mm/day) over large areas. Existing methods are predominantly dependent on Non-Remote Sensing approaches, based on point climate data and/or official database and statistics. Given the above background, the main aim of this study was to develop daily Evapotranspiration image/map by estimating actual crop evapotranspiration for irrigation designing, scheduling and planning, water resource management and cropping system modeling using thermal band data of LANDSAT 7ETM+ and surface energy balance model.

## 2. STUDY AREA

The Hansi Branch Canal Command, a part of the Western Yamuna Canal (WYC) command takes off from the main branch (WYC) at Munak distribution head work near village Munak (Karnal District) and supply irrigation to Karnal, Jind and Hisar districts of Haryana. It is located Approximately between 29°43' to 29°51' North Latitude and

75°53' to 76°45' East longitude. The study area falls in semi-arid climate with mean annual rainfall of 515mm and mean maximum temperature is 41°C (May and June) and mean minimum is 6°C(January)

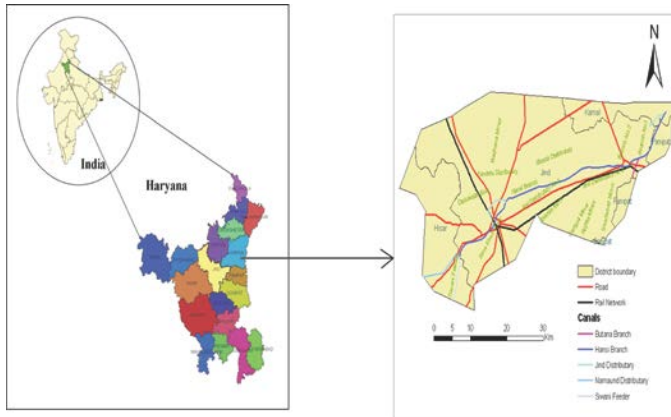


Figure 1: Location and major canals and features of the study area

Table 1: Information on satellite and sensor characteristics

Satellite and sensor	Band	Spectral resolution (μm)	Spatial resolution (meters)
LANDSAT-7 ETM +	1	0.45 - 0.53	30
	2	0.52 - 0.60	30
	3	0.63 - 0.69	30
	4	0.77 - 0.90	30
	5	1.55 - 1.75	30
	6	10.40 -	60
	7	12.50	30
	8	2.09 - 2.35	15
			0.52 - 0.90

**WEATHER DATA:** Weather data for a representative station was obtained from Agro-met observatory CSSRI, Karnal. The weather conditions prevailing on 11th March 2002 are in Table 2. The wind speed (u) at the time of the satellite overpass was also acquired for the computation of sensible heat flux (H) and for the ETr calculation. In addition to it, information about water resource, irrigation supply, irrigated crops and irrigated land area were also collected. Hourly and daily data were used in SEBAL processing.

### 3. MATERIALS AND METHODS

**Satellite Data:** Landsat 7ETM+, which began operation in March 2002 view the entire earth surface over 16 days; acquire data in eight spectral bands (different wavelengths of electromagnetic radiation). These bands have 30m spatial resolution. The single date image of 11th March 2002 (details in Table 1) was used for determination of different components of surface energy balance.

**Table 2: Weather conditions at the time of satellite overpass on the study area**

Satellite Overpass date: (11 March 2002) Local time: 10.20AM						
Parameters	Air temperature (°C)	Relative humidity (%)	Wind speed (km/hr)	Daily Sunshine (hours)	Precipitation (mm)	Pan evaporation (mm)
11 March 2002	19.6	32	4.0	9.3	0.0	03.7
12 March 2002	17.5	65	4.5	9.5	0.0	03.9

**Running SEBAL:** The Surface Energy Balance Algorithm for Land (SEBAL) is a parameterization of the energy balance and surface fluxes based on spectral satellite measurements (Bastiaanssen et al. 1999). In the SEBAL model, ET is computed from satellite images and weather data using the surface energy balance. Since the satellite image provides information for the overpass time only, SEBAL computes an instantaneous ET flux for the image time. The ET flux is calculated for each pixel of the image as a “residual” of the surface energy budget equation. The principles and steps needed to apply SEBAL to estimate evapotranspiration are described in Bastiaanssen (1995), Bastiaanssen et al. (1998).

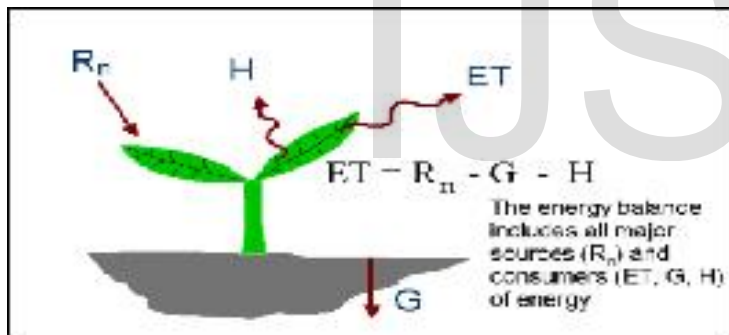


**Figure 2: Surface energy balance in SEBAL**

Evapotranspiration (ET) is computed as a residual of the energy balance equation on a pixel-by-pixel basis:

$$\lambda * ET_{pixel} = LE_{pixel} = R_{pixel} - H_{pixel} - G_{pixel} \dots \dots (1)$$

where  $LE_{pixel}$  : latent heat flux for the pixel,  $ET_{pixel}$  : pixel evapotranspiration ET,  $\lambda$ : latent heat of vaporization, and  $R_{pixel}$ ,  $H_{pixel}$  and  $G_{pixel}$  are the net radiation, sensible heat flux and soil heat flux for each pixel, respectively.

The net radiation flux at the surface ( $R_n$ ) represents the actual radiant energy available at the surface. It is computed by subtracting all outgoing radiant fluxes from all incoming radiant fluxes (Figure 6). This is given in the surface radiation balance equation:

$$R_n = R_s \downarrow - \alpha R_s \downarrow + R_L \downarrow - (1 - \epsilon_0) R_L \downarrow \dots \dots (2)$$

$R_s \downarrow$  is incoming shortwave radiation ( $W/m^2$ ),  $\alpha$  is broadband surface albedo (dimensionless),  $R_L \downarrow$  is incoming longwave radiation ( $W/m^2$ ),  $R_L \uparrow$  is outgoing long wave radiation ( $W/m^2$ ),  $\epsilon_0$  is surface thermal emissivity (dimensionless),  $R_n$  represents the actual radiant energy available at the surface ( $100-700 W/m^2$ ).

$$\text{Net surface radiation} = \text{gains} - \text{losses} \dots \dots (3)$$

In Equation (2), the amount of shortwave radiation ( $R_s \downarrow$ ) that remains available at the surface is a function of the surface albedo ( $\alpha$ ).

Surface albedo is a reflection coefficient defined as the ratio of the reflected radiant flux to the incident radiant flux over the solar spectrum. It is calculated using satellite image information on spectral radiance for each satellite band. The incoming shortwave radiation ( $R_s \downarrow$ ) is computed using the solar constant, the solar incidence angle, a relative earth-sun distance, and a computed atmospheric transmissivity. The incoming long wave radiation ( $R_L \downarrow$ ) is computed using a modified Stefan-Boltzmann equation with atmospheric transmissivity and a selected surface reference temperature. Outgoing long wave radiation ( $R_L \uparrow$ ) is computed using the Stefan-Boltzmann equation with a calculated surface emissivity and surface temperature. Surface temperatures

are computed from satellite image information on thermal radiance. The surface emissivity is the ratio of the actual radiation emitted by a surface to that emitted by a black body at the same surface temperature. In SEBAL, emissivity is computed as function of vegetation index. The final term in Equation (2),  $(1 - \epsilon_o) R_{L\downarrow}$ , represents the fraction of

incoming long wave radiation that is lost from the surface due to reflection.

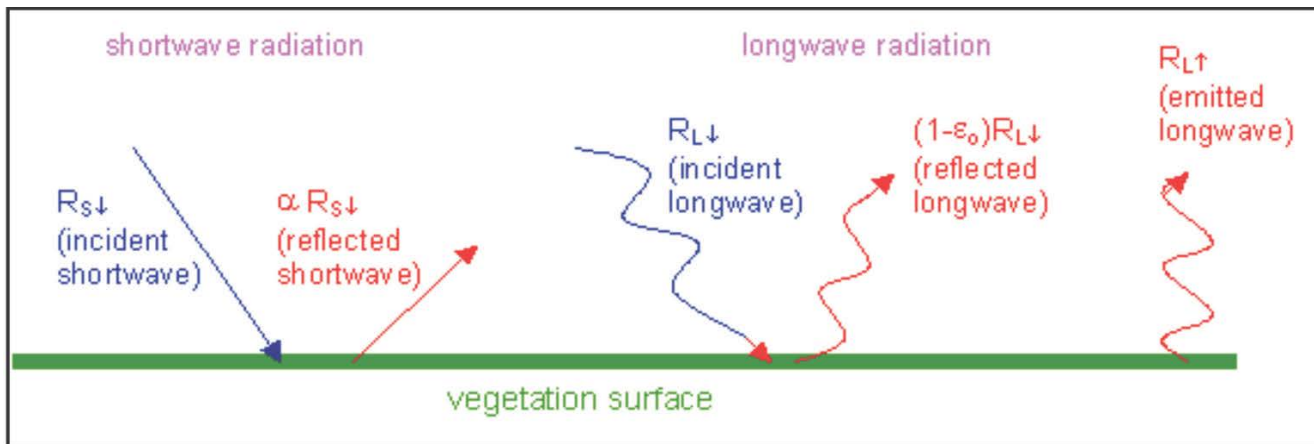


**Figure 3: Surface radiation balance in short and long wavelength**

Soil heat flux cannot be directly determined from satellite sensors and requires empirical formulation. Remote Sensing derivable parameters that influence soil heat flux are used; these include NDVI, surface temperature and albedo. The soil heat flux (G) has been estimated using the following empirical equation proposed by Bastiaanssen (2000) for any condition of vegetation cover and type of soil is

$$\frac{G}{R_n} = \frac{T_s}{\alpha} (0.0038\alpha + 0.0074\alpha^2)(1 - 0.98NDVI^2) \dots \dots \dots (4)$$

Where, G: soil heat flux,  $T_s$  : surface albedo,  $T_s$ : surface temperature (°C), and NDVI: normalized difference vegetation index. NDVI is calculated from the Landsat band 4 and band 3 reflectances ( $\rho_4$  and  $\rho_3$ , respectively) as  $NDVI = (\rho_4 - \rho_3) / (\rho_4 + \rho_3)$ ; NDVI values normally range from 0 to 1, where a  $NDVI > 0.7$  represents full cover conditions for most crops.

A considerable amount of solar radiation reaching the earth's surface is reflected. The fraction  $\alpha$ , of the solar radiation reflected by the surface is termed as the albedo. The albedo is highly variable for different surfaces and for the angle of incidence or slope of the ground surface.

After calculating  $R_n$  and G, the calculation of the sensible heat flux, H, is required to obtain the parameters that will allow the computation of ET as a residual from the energy balance. The aerodynamic transfer of heat to air, H, is predicted using the following equation (Brutsaert, 1982):

$$h(x, y) = \rho C_p \left[ \frac{T_{aero} - T_a}{r_{ah}} \right] \dots \dots \dots (5)$$

where,  $\rho$  is air density, a function of atmospheric pressure;  $C_p$  is specific heat capacity of air;  $T_{aero}$  is aerodynamic surface temperature;  $T_a$  is reference height air temperature; and  $r_{ah}$  is aerodynamic resistance to sensible heat transport between the surface and the reference height. Accurate application of Equation (21) from satellite data is hindered by the difficulty in estimating aerodynamic surface temperature ( $T_{aero}$ ) accurately, due to uncertainty in atmospheric attenuation, contamination and radiometric calibration of the sensor, and because radiometric temperature  $T_s$ , as measured by satellite, deviates from aerodynamic temperature  $T_{aero}$  that derives the heat transfer process.

In SEBAL, instead of  $T_{aero}$ , the reference temperature is taken to be  $T_1$ , an air temperature located at height  $z_1$  close to surface ( $z_1 = 0.1$  m). An upper height is taken at a height  $z_2 = 2$  m and its corresponding temperature is called  $T_2$ . The difference between  $T_1$  and  $T_2$  is referred as the "near surface air temperature difference" or  $dT$ . The sensible heat flux is then defined as

$$H = \frac{\rho \times C_p \times dT}{r_{ah}} \dots \dots \dots (6)$$

where,  $r_{ah}$  is aerodynamic resistance to heat transport between  $z_1$  and  $z_2$ , and  $dT$  is air temperature difference between the two heights  $z_1$  and  $z_2$  above the surface,  $dT = T_1 - T_2$ .

To determine the value of  $dT$  for each pixel, the SEBAL procedure assumes the existence of a linear relationship between  $dT$  and the surface temperature  $T_s$ :

$$dT = aT_s + b \dots \dots \dots (7)$$

where,  $T_s$  : radiometric surface temperature, and "a" and "b": empirical coefficients obtained from the so - called "anchor" pixels (Bastiaansen,1995). The assumption implicit in the SEBAL is that hot areas (with large emittance) create a higher vertical  $dt$  than cold surfaces, and that this relationship is linear.

In summary, SEBAL is applied following these steps:

#### 4. RESULTS & DISCUSSION

The Landsat-7 ETM+ digital data in the visible, infrared and thermal infrared bands was used in SEBAL to generate the images of surface albedo ( $\alpha$ ), surface temperature ( $T_s$ ), normalized difference vegetation index (NDVI), net surface radiation (Rn), soil heat flux (G) and sensible heat flux(H), to calculate the spatial ETa.

For the study area, the surface albedo ( $\alpha$ ) was estimated and ranged between 0.10 and 0.43 with its mean value of 0.26. The highest value was observed in bare soil surface (Figure 4). The light blue colour representing built-up land has high surface albedo. The NDVI was estimated that ranged between -0.11 and 0.81 and the mean is 0.468. The highest value was found in the agricultural lands (Figure 5) by the dark green color. The lighter gray shade shows the lowest value of NDVI in the built up land. The high NDVI was considered as an indicative of maximum ground cover by agricultural crop. The surface temperature ( $T_s$ ) was in the range of 15 - 70°C and the mean  $T_s$  was calculated to be 27°C. It is seen (Figure 6) that the agricultural area

- a) calculation of Rn for each pixel from Eq. 2
- b) calculation of G for each pixel from Eq. 3;
- c) definition of the  $dT$  function (Eq. 6) using  $dT$  and  $T_s$  obtained from the two "anchor" pixels;
- d) calculation of  $dT$  for each pixel from the pixel surface temperature, using Eq. 6;
- e) calculation of H for each pixel from Eq. 5; and
- f) calculation of LE (ET) from Eq.1.

All energy balance fluxes (Rn, G, H, and LE) represent instantaneous fluxes corresponding to the instant when the satellite image was taken.

represented by dark green color lies in medium range of surface temperature that range between 27°C and 70°C. Whereas the rust shade represented by built up land inclusive of water bodies shows lower range of temperature.

The above mentioned parameters are important in the calculation of Net Surface Radiation (Rn) and Soil Heat flux (G). The Rn flux ranged between 166.2 and 1195.8 W/m<sup>2</sup> and the mean Rn was 729.0 W/m<sup>2</sup>. It can be seen that water bodies were having high Rn values whereas dry areas were observed with low Rn fluxes (Figure 7). For the cropped area, Rn was observed between 318-420 W/m<sup>2</sup>. The range of G flux was observed between 48.3 and 173.2 W/m<sup>2</sup> and the mean for G was 99.6 W/m<sup>2</sup> for the Hansi Branch Canal Command (Figure 8). As per the statistics, the high values of G were observed in agricultural area followed by plantation, whereas the low G fluxes were observed from built up lands mostly surrounded by community grass/grazing land. The Sensible Heat Flux (H) image for the study area computed and is shown in (Figure 9). The statistical analysis of the image indicates that H was ranging

between 68.8 and 87.5 W/m<sup>2</sup> and the mean was calculated to be 81.82 W/m<sup>2</sup>. For the agricultural areas, H flux was observed between 74 and 79.0

W/m<sup>2</sup> and for the built-up areas was observed to be more than 80.0 W/m<sup>2</sup>.

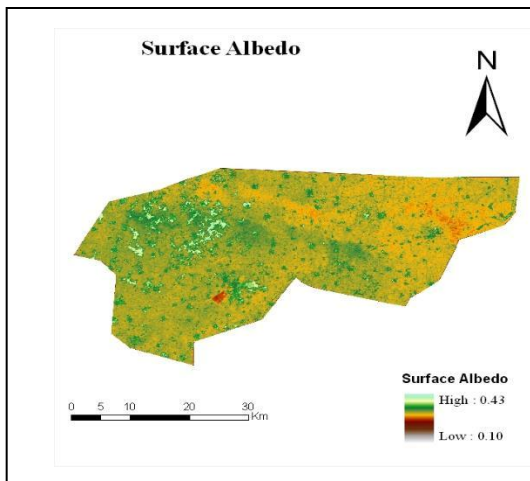


Figure 4: Surface albedo image

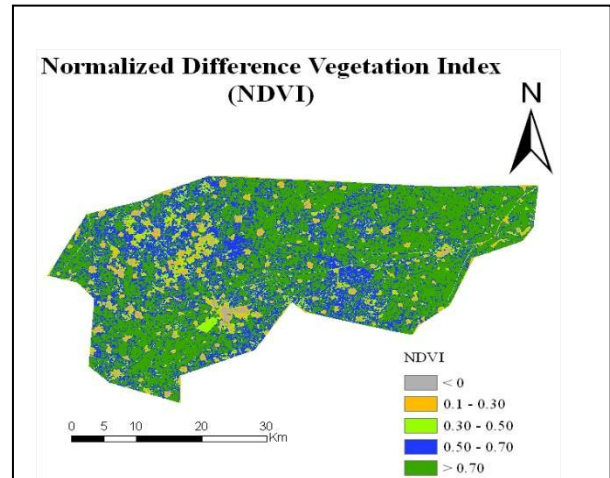


Figure 5: NDVI image

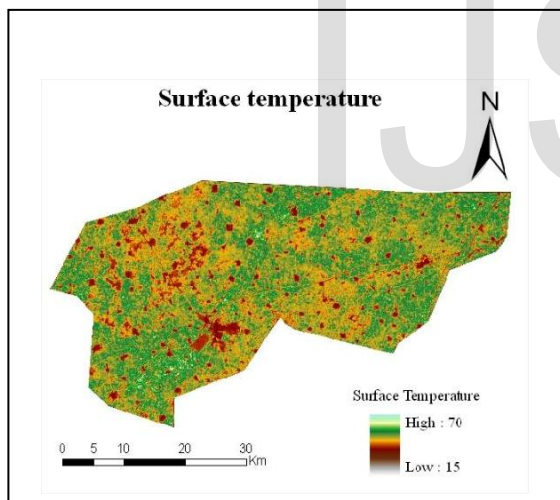


Figure 6: Surface temperature image

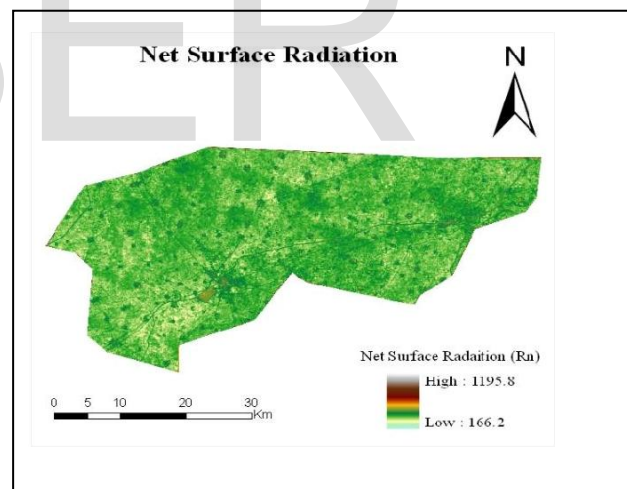


Figure 7: Net Surface radiation image

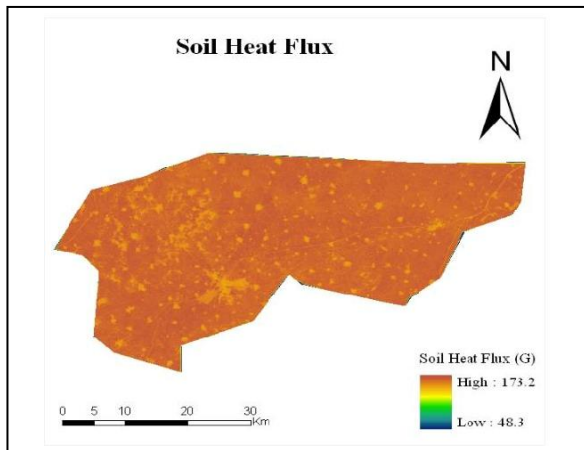


Figure 8: Soil heat flux image

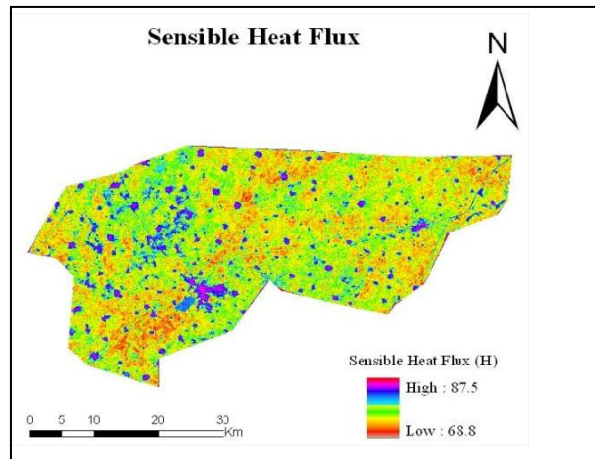


Figure 9: Sensible heat flux image

The instantaneous  $\lambda E$  fluxes were computed and these values were then converted to 24 hour evapotranspiration rate. The ET was ranging between 0.05 to 3.48 mm/day and the mean was 1.13 mm/day. The value for highest ET was reported in the water bodies of 3.48 mm/day, inclusive of large and small water bodies that consist of multiple mixed pixels falling both on land as well as averaging differences in the water surface temperature due to turbidity. For the cropped areas, it was observed between 0.06 and 2.53 mm/day. The lower values were for those pixels in the image which shows highest range of temperature in the agricultural land (Figure 10) and the ET value ranges more than 0.5 mm/day were for fallow area means

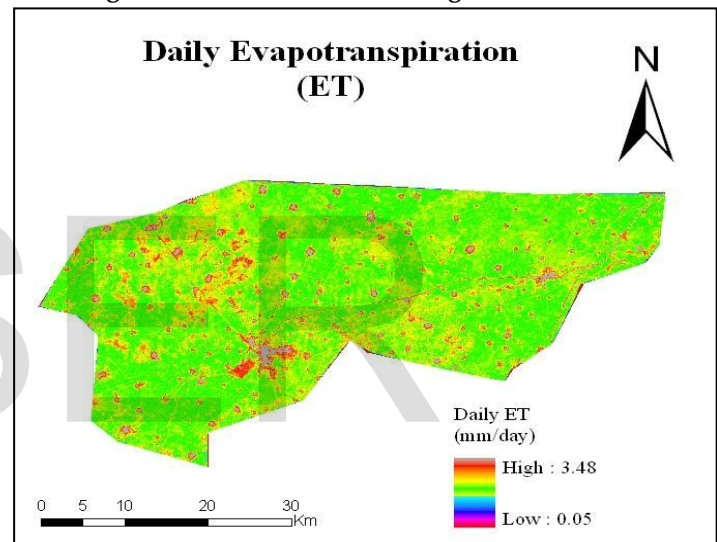


Figure 10: Daily evapotranspiration image

agricultural area used during Kharif period. Exclusive wheat crop area shows the higher range of ETa that varies between 1.44 to 2.53 mm/day. For the built-up area and other land use like community grass/ grazing land and plantation, it was observed less than 1.0 mm/day.

**Comparison of Results:** The model results were evaluated with the ETc estimated from two widely used methods, Pan-Evaporation method and Penman-Monteith method. Both method, are commonly used for irrigation scheduling in field and research farm experimentation. Both the conventional methods provide a measurement of the combined effect of temperature, humidity, wind speed and sunshine on the reference crop evapotranspiration (ETo) and crop and soil

conditions on ETc. The pan evaporation values are reported in Table 2

The average ETa value from the SEBAL model for wheat crop over the study area was 2.17 mm/day. The ETc values of wheat crop estimated using Pan-Evaporation method and Penman-Monteith method for 11 March were 2.50 mm/day and 3.26 mm/day, respectively. The model predicted ETa is 15.1% less than ETc estimated from the first method and 50.2% less than ETc estimated from the second method. This large variation of actual evapotranspiration of wheat from the SEBAL is due to various wheat crop conditions resulting from the multiple dates of sowing between 15 November and 15 December observed in the study area due to late

harvesting of rice and cotton. Moreover, functioning of many brick kilns in the study area may have increased surface temperature of surrounding pixel leading to low actual ET. The evaluation results with two conventional methods showed that the SEBAL model has the close performance with widely accepted Pan Evaporation method for irrigation scheduling, but

## CONCLUSION

The following conclusions have been drawn from this study.

- The SEBAL model, a physically based surface energy balance model was found to be suitable for partitioning of surface energy into various energy components for computing accurate estimates of spatial ET for aggregating crop water requirement at distributary and branch canal level.
- The image for daily evapotranspiration shows the ETa values for all land use categories. The ETa values for agricultural area range between 0.06 and 2.53 mm/day. The water bodies show the highest ET range more than 1.5 mm/day whereas ETa for built-up area and plantation was observed less than 1 mm/day. The wheat crop area shows the higher range of ETa that varies between 1.44 to 2.53 mm/day

## REFERENCES

Allen, R.G., Tasumi, M., Morse, A. and Trezza, R. (2005). A Landsat-based energy balance and evapotranspiration model in Western US water rights regulation and planning. *Irrigation and Drainage Systems*, 19 (3-4), 251-268.

Ahmad, M.D., Biggs, T., Turrall, H. and Scott, C.A. (2006). Application of SEBAL approach and MODIS-time-series to map vegetation water use patterns in the data scarce Krishna River Basin of India. *Water Science & Technology*, 53 (10), 83-90.

Bandara, K.M.P.S. (2006). Assessing irrigation performance by using remote sensing. Doctoral

has large variation from the Penman-Monteith method which might over predict the crop evapotranspiration considering uniform crop conditions which is not true in fields. Therefore, SEBAL model can be recommended for estimation of the spatial ETa for crop water demand management

- The results obtained from the SEBAL model were compared with the results estimated from two conventional methods i.e. Pan Evaporation and Penman - Monteith. The results found close to the results obtained from Pan-Evaporation method with 15 % variation, but large variation (50%) with the results obtained from the Penman - Monteith method. The comparison has also revealed a reasonable estimate of daily evapotranspiration for peak season through SEBAL. This indicates reasonably acceptable spatial estimates of distributed daily evapotranspiration by the model.
- Satellite Remote Sensing techniques with the limited ground data is a reliable approach to estimate the crop water demands that in turn, help for planning the efficient operational schedule for the Hansi Branch Canal in the WYC Command.

Thesis, Wageningen University, Wageningen, The Netherlands.

Bastiaanssen, W.G. M. (1995). Regionalization of surface flux densities and moisture indicators in composite terrain. Doctoral Thesis, Agricultural University, Wageningen, The Netherlands.

Bastiaanssen, W.G.M., Menenti, M.R., Feddes, A., and Holtslag, A.M. (1998). A remote sensing surface energy balance algorithm for land (SEBAL): 1. Formulation. *Journal of Hydrology*, 198-212.

Bastiaanssen, W.G.M., Pelgrum, H., Wang, J., Ma, Y., Moreno, J.F., Roerink, G.J., Wal, T. (1998). A remote sensing surface energy balance algorithm for land

(SEBAL) : 2. Validation. *Journal of Hydrology*, 213-229.

Bastiaanssen, W. G. M., Molden, D. J. and Makin, I. W.



(2000). Remote sensing for irrigated agriculture: Examples from research of possible applications.

Agricultural Water Management, 46(2), 137-155.

Bastiaanssen, W.G.M., Harshadeep, and Rao, Nagaraja (2005). Managing scarce water resources in Asia: The nature of the problem and can remote sensing help? Irrigation and Drainage Systems, 19, 269-284.

Bastiaanssen, W.G.M., Noordman, E.J.M., Pelgrum, H., Davids, G., Thoreson, B.P. and Allen, R.G. (2005). SEBAL model with remotely sensed data to improve water-resources management under actual field conditions. J. Irrig. Drain. Engg, 131, 85-93.

Courault, D., Seguin, B. and Olioso, A. (2005). Review on estimation of evapotranspiration from remote sensing data: From empirical to numerical modeling approaches. Irrigation and Drainage Systems, 19 (3-4), 223-249.

CWC (1998). Status Report on Evaporation Control in Reservoirs. Central Water Commission, New Delhi.

Doorenbos, J. and Pruitt, W.O. (1977). Crop Water Requirements. Irrigation & Drainage Paper No. 24 (revised), FAO, Rome, Italy.

Engman, E.T. and Gurney, R.J. (1991). Remote Sensing in Hydrology, Chapman and Hall, London, U.K.

FAO (2005), Crop Water Needs, Chapter 3. ([www.fao.org/docrep/s2022E/s2022e07/](http://www.fao.org/docrep/s2022E/s2022e07/)), Access date: 6th June, 2011.

Gontia, N.K. and Tiwari, K.N. (2004). Estimation of crop coefficient and evapotranspiration of wheat (*Triticum aestivum*) in an irrigation command using remote sensing and GIS. Water Resources Management, Manuscript No. WARM9442.

Hafeez, M. and Khan, S. (2004). Remote sensing application for estimation of irrigation water consumption in Liuyuan irrigation system in China. CSIRO Land & Water Division and School of Science & Technology, Charles Sturt University, Australia.

Kumar, M. Dinesh, Sivamohan, M.V.K. and Narayanamoorthy, A. (2003). Food security and sustainable

agriculture in India: The water management challenge, IWMI Paper 60, International Water Management Institute, (Colombo).

Kustas, W.P. and Norman, J.M. (1996). Use of remote sensing for evapotranspiration monitoring over land surface. Hydrological Sciences Journal, 41(4), 495-516

Lillesand, T. and Kiefer, R. (2004). Remote Sensing and Image Interpretation. John Wiley & Sons, Inc. 5th edition, New York.

NRAA (2010). Food security, Water and Energy nexus in India, Draft Policy paper, National Rainfed Area Authority (NRAA), New Delhi.

([www.nraa.gov.in/Food\\_Security\\_Water\\_And\\_Energy.pdf](http://www.nraa.gov.in/Food_Security_Water_And_Energy.pdf)), Access date: 26th May, 2011).

Tanwar, R.S. and Kruseman, G.P. (1985). Hydrogeology in the Services of Man, Memoires of the 1861 Congress of the International Association of Hydrogeologists, Cambridge.

Thiruvengadachari, S. (1996). Assessing Irrigation Performance of Rice-Based Bhadra Project in India. <http://www.gisdevelopment.net/aars/acrs/1996/ts1/ts1008.shtml>, Access date: 4th May, 2011.

Water Watch, (1998). Remote Sensing Services for Quantifying Water Management. [www.waterwatch.nl](http://www.waterwatch.nl)

Li, Zhao - Liang, Ronglin, Tang, Zhengming, Wan, Yuyun, Bi, Chenghu, Zhou, Bohui, Tang, Guangjian, Yan and Xiaoyu, Zhang (2009). A review of current methodologies for regional evapotranspiration estimation from remotely sensed data. Sensors, 9, 3801-3853.